Methods 65 (2014) 247–253

Contents lists available at ScienceDirect

Methods

journal homepage: www.elsevier.com/locate/ymeth

Zebrafish as a model to study PTPs during development

Jeroen Paardekooper Overman [a], Jeroen den Hertog [a,b,*]

[a] Hubrecht Institute-KNAW and University Medical Centre Utrecht, The Netherlands
[b] Institute of Biology Leiden, Leiden University, The Netherlands

ARTICLE INFO

Article history:
Available online 22 August 2013

Keywords:
Protein-tyrosine phosphatase
Zebrafish
Gastrulation cell movements
Phosphoproteomics
Phosphotyrosine

ABSTRACT

Protein-tyrosine phosphatases (PTPs) have important roles in signaling, but relatively little is known about their function *in vivo*. We are using the zebrafish as a model to study the function of PTPs at the organismal, cellular and molecular level. The zebrafish is an excellent experimental model for the analysis of gene function. We have developed methods to quantitatively study effects of PTP knockdown or expression of (mutant) PTPs, particularly with respect to gastrulation cell movements. Moreover, we have studied the phosphoproteome of zebrafish embryos. In this review, we will discuss methods to manipulate the zebrafish genome and techniques that we have developed to assess developmental defects during gastrulation and to assess differences in the phosphoproteome.

1. Introduction

Much is known about catalysis and regulation of PTPs [44]. However, to fully understand the function of PTPs, their role in whole organisms *in vivo* needs to be addressed. Several model organisms have been used to investigate the function of PTPs, including the invertebrates *Drosophila* and *Caenorhabditis.elegans* and vertebrate models, particularly the mouse. Many mouse knock-outs have been generated that provided important insight into the function of PTPs in development and conditional knock-outs have allowed the analysis of the function of PTPs in particular tissues [18,19]. Generation of mouse models can be laborious however, and *in vivo* imaging is difficult. We and others have used the zebrafish as a model for the analysis of PTP function, because of the many advantages that zebrafish embryos have to offer as an experimental system. Zebrafish are particularly amenable for genetics, intravital imaging and large scale approaches. In addition, we have recently developed a method to derive cell lines from single zebrafish embryos and tumors [10], which complements the wide range of experimental approaches in zebrafish. Here, we will review zebrafish as a model system in general, the genetic tools available, the approaches that we have used to assess PTP function in zebrafish, focusing on *in vivo* cell behavior and phosphoproteomics and we will give an outlook on approaches that may be used in the near future to assess PTP function *in vivo*.

2. Zebrafish as an experimental system

The zebrafish is an excellent model system that was initially used for large scale forward genetic screens [13,16]. Since then, zebrafish are increasingly being used to model human diseases [35]. Major advantages of the zebrafish as an experimental system are that large numbers of embryos can be obtained easily; 100–200 embryos per clutch, 1–2 clutches per week per adult zebrafish pair. The embryos develop quickly and outside the mother; after 1–2 days most organs have formed. The embryos are transparent, facilitating analysis of embryonic development by (time-lapse) microscopy. Many genetic mutants are available and transgenesis is feasible. More and more transgenic lines are becoming available, expressing fluorescent marker proteins under the control of specific promoters, which allows for intravital imaging. Overexpression of genes or proteins of interest can easily be achieved by micro-injection of synthetic mRNA encoding the protein of interest at the one-cell stage. In addition, transient knockdown of target proteins and target-selected gene inactivation are feasible in zebrafish (see below). Finally, chemical compounds can easily be administered to zebrafish embryos by simple addition to the aqueous embryo medium. Medium to large scale screens for bioactive compounds have been done using zebrafish development as read-out [11,38]. Taken together, the zebrafish is an ideal model system for analysis of gene function at the genetic, molecular and cellular level in whole organisms.

3. Zebrafish protein tyrosine phosphatases

The zebrafish genome sequence is available in public databases (http://www.ensembl.org/Danio_rerio/Info/Index) [20]. In general, orthologs of most human genes can be found in the zebrafish

* Corresponding author at: Hubrecht Institute, Uppsalalaan 8, 3584 CT Utrecht, The Netherlands.
E-mail address: j.denhertog@hubrecht.eu (J. den Hertog).

1046-2023/$ - see front matter © 2014 Published by Elsevier Inc.
http://dx.doi.org/10.1016/j.ymeth.2013.08.018

genome. In fact, some genes are duplicated in the zebrafish genome, due to a genome duplication in teleosts 320 million years ago [22,48]. In human, PTPs are divided in four classes i.e. classical and VH1-like dual specific protein phosphatases (DSPs) (class I), low molecular weight phosphatases (class II), Cdc25 phosphatases (class III) and Aspartic acid–based pTyr specific phosphatases (IV) [2]. Class I classical PTPs are further subdivided into receptor and non-receptor PTPs. Class I DSPs are divided into seven groups, namely: mitogen activated protein kinase (MAPK) phosphatases (MKPs), atypical DSPs, the slingshot phosphatases, PRLs, CDC14s, phosphatase and tensin homologues (PTENs) and myotubularins. Since we focus on classical PTPs and PTENs, these will be discussed in this review.

The zebrafish genome encodes 51 classical PTPs and all the subtypes that have been identified in the mammalian genomes are represented in the zebrafish genome [45] (Table 1). Fourteen PTP genes are duplicated in the zebrafish genome and whether these duplicated genes are all functional remains to be determined. Comparison of the PTP family in the genome of five distinct fish species led to the surprising discovery that *ptpn20*, which was supposed to encode little more than a PTP domain, actually encodes a large PTP with multiple functional domains, resembling PTP-BL. The human and mouse *ptpn20* genes have a similar structure as zebrafish *ptpn20*, and we confirmed this by reverse transcription PCR [46].

To unravel the function of PTPs during zebrafish development, we have compared the expression patterns of all PTP genes in zebrafish by whole mount *in situ* hybridization using standard protocols [43,45]. Most PTP genes are expressed throughout development with broad expression patterns early on, which become more restricted later in development [45]. Interestingly, some of the duplicated PTP genes have overlapping spatio-temporal expression patterns whereas others are mutually exclusive. It is likely that the function of the latter PTPs has diverged since their duplication. For gene specific expression data during embryonic development we refer to [45].

4. Genetic tools to study PTP function in zebrafish

PTP function has been studied in zebrafish by transient, morpholino-mediated knockdown, in genetic loss-of-function mutants and by expression of exogenous PTP genes and mutants thereof.

4.1. Morpholinos

Transient knockdown of target proteins by microinjection of morpholinos is widely used to study gene function [29,337]. Morpholinos are either directed at the start ATG to block translation of the target protein or at splice sites to block splicing of the target RNA (Fig. 1). Morpholino-mediated knockdown of Pez (*ptpn14*) results in developmental defects in the heart and somites, which may at least in part be mediated by impaired TGFβ3 signaling-dependent epithelial to mesenchymal transition [52]. Knockdown of PTPσ results in accumulation of synaptic vesicles in the axon terminals of olfactory sensory neurons [8]. PTPσ is related to the LAR receptor tyrosine phosphatases and these guide peripheral sensory axons to the skin in zebrafish embryos [50]. Ve-ptp is required for vascular integrity, due to its role in adherens junctions where it regulates VEGFR-dependent VE cadherin phosphorylation and cell polarity [6,17]. Ptpro is structurally related to Ve-ptp and is required for cerebellar formation [32]. Knockdown of Shp1 (*ptpn6*) hyperactivates the innate immune system [26]. All of the studies above used transient morpholino-mediated knockdown of the PTP target proteins. To study the function of all classical PTPs in development, we have designed two non-overlapping morpholinos against each classical PTP gene in the zebrafish genome and assessed their effects on early development by micro-injection at the one-cell stage. Not all pairs of morpholinos induced the same defects, suggesting off-target effects [47]. We have pursued some knockdowns in detail (see below) and rescue of the morpholino-induced defects by co-expression of the respective target RNAs is taken as good evidence that the observed defects are not merely off-target effects.

4.2. Target selected gene inactivation

Off-target effects of morpholinos are a concern and reverse genetics approaches have been developed to generate genetic mutants of target genes. Both mutagenesis and viral insertions are commonly used to disrupt target genes. Many loss-of-function mutations have been identified in PTP genes (www.zfin.org) (Table 1). Mutagenesis-based gene inactivation makes use of reagents such as N-ethyl-N-nitrosourea (ENU) to generate random single nucleotide polymorphisms (SNPs) in adult males. Subsequently, offspring is generated and mutations are identified in target genes by SNP detection or sequencing. Target selected gene inactivation by random mutagenesis and resequencing of the gene of interest in a large number of F1 mutants has led to the identification of nonsense mutations in more than 200 target genes [51] (www.zfin.org). An ongoing project makes use of high-throughput sequencing and is aimed at disrupting every gene in the zebrafish genome. So far potentially disruptive mutations have been identified in 38% of the zebrafish genes [28].

One of the first genes that were disrupted by the original target selected gene inactivation method was zebrafish *pten*. PTEN is a prominent member of the PTP superfamily, even though its catalytic activity is directed at lipids, rather than phosphotyrosine. *PTEN* is one of the most frequently mutated tumor suppressor genes in human cancer and is essential for mammalian development. We identified an early stop in the *pten* gene and much to our surprise, homozygous fish were viable. However, unlike the human genome, the zebrafish genome encodes two *pten* genes, *ptena* and *ptenb*, prompting us to disrupt the second *pten* gene too. Zebrafish embryos without functional Pten ($ptena^{-/-}ptenb^{-/-}$) display various hyperplastic/dysplastic defects and are embryonic lethal [14]. Genetic mutants that lack functional Ptena or Ptenb are viable and fertile, indicating that Ptena and Ptenb have at least partially redundant functions. Yet, adult fish that retain only a single wild type *pten* allele ($ptena^{+/-}ptenb^{-/-}$ and $ptena^{-/-}ptenb^{+/-}$) develop hemangiosarcomas, endothelial tumors [9]. These findings illustrate that the duplication of genes in teleosts can be used to study gene function in a way that is not possible in mammalian systems. Future analysis of the *pten* mutants will provide new insights into Pten function *in vivo*.

4.3. Gene targeting

Specific gene inactivation by directing nuclease activity to target genes has been developed successfully for zebrafish as well. Zinc Finger Nuclease (ZFN) technology has been used [12,36] and more recently, Transcription Activator Like Effector Nuclease (TALEN) technology appears even more successful [5]. Clustered Regularly Interspaced Short Palindromic Repeat (CRISPR)-associated systems (Cas) technology has also been applied to inactivate genes in zebrafish [21] and holds much promise for future inactivation of target genes. All nuclease technologies are based on the generation of double-stranded breaks in the target gene, which are repaired by endogenous DNA repair mechanisms, particularly non-homologous end-joining (NHEJ). NHEJ frequently makes mistakes, leading to short deletions and these actually result in frame shifts and hence inactivation of the target genes. In principle, a template can be provided exogenously for DNA repair by homologous recombination, facilitating the introduction of (disease-associated)

Table 1
Zebrafish phosphatases. The zebrafish genes, their protein names and the human orthologues are depicted here with phenotypes described in fish, genetic associations and available mutant zebrafish lines. Genetic associations are derived from the Genetic Association Database: http://geneticassociationdb.nih.gov/cgi-bin/index.cgi. Not all genetic associations are mentioned here due to space constrictions. Data describing Single Nucleotide Polymorphisms (SNPs) from mutagenesis screens and transgenic insertions disrupting gene function [49] are derived from www.zfin.org. + indicates single SNP or transgenic insertion, ++ indicates two SNPs or transgenic insertions etc. – indicates no SNP or transgenic insertion was identified in this gene. Further details of transgenics and zebrafish phenotypes are described in the text.

Zebrafish gene	Zebrafish protein	Human protein	Subtype	Phenotype in fish	Genetic association database	SNP (ZFIN)	Tg insertion (ZFIN)
ptpn1	PTP1b	PTP1B	NT1	–	Diabetes type 1 and 2; obesity	–	–
ptpn2a, ptpn2b	tcPTPa, tcPTPb	TCPTP	NT1	–	Diabetes type 1; Celiac disease; Crohn's disease; Lupus	–	
ptpn3	PTPh1	PTPH1	NT5	–	Neuroblastoma; Albumins; Echocardiography	–	+
ptpn4a, ptpn4b	meg1a, meg1b	MEG1	NT5	–	–	+	–
ptpn5	PTP-STEP	PTP-STEP	R7	–	–	–	–
ptpn6	shp1	SHP1	NT2	Immune system [26]	–	–	–
ptpn7	HePTP	HePTP	R7	–	–	–	–
ptpn9a, ptpn9b	meg2a, meg2b	MEG2	NT3	–	Height; (Embryonic lethality in mouse)	+	+
ptpn11a, ptpn11b	shp2a, shp2b	SHP2	NT2	Gastrulation; Noonan and LEOPARD syndrome [25]	Leukemia; Noonan and LEOPARD syndrome; Platelet count	+	+
ptpn12	PEST	PTPPEST	NT4	–	Insulin	–	–
ptpn13	PTPBAS	PTPBAS	NT7	Gastrulation [46]	Cardiovascular	+	+++
ptpn14	PTP36	PTP36	NT6	Heart, somite [52]	ADD; blood cells; blood flow velocity	–	–
ptpn18	BDP1	BDP1	NT4	–	–	–	–
ptpn20	PTPTyp	TYP	NT8	Gastrulation [46]	–	+	+
ptpn21	PTPd1	PTPD1	NT6	–	Schizophrenia	+	–
ptpn22	LyPTP	LyPTP	NT4	–	Diabetes type 1 and 2; Rheumathroid arthritis;	+	–
ptpn23a, ptpn23b	hdPTPa, hdPTPb	HDPTP	NT9	–	Cell invasion	+	–
ptpra	RPTPα	RPTPα	R4	Gastrulation [45]	–	++	++
ptprb	RPTPβ	RPTPβ	R3	Vascular integrity [6,17]	Calcium	–	+++
ptprc	CD45	CD45	R1/R6	–	Multiple sclerosis; lupus erythematosus	+	+ (dsRed)
ptprda, ptprdb	RPTPδa, RPTPδb	RPTPδ	R2B	–	Diabetes; Cholesterol; Coronary disease; Heart failure	+++++	+
ptprea, ptpreb	RPTPεa, RPTPεb	RPTPε	R4	Gastrulation [45]	Coronary disease; Ewing sarcoma	++	+
ptprfa, ptprfb	LARa, LARb	LAR	R2B	Peripheral sensory axons [50]	–	+++	++
ptprga, ptprgb	RPTPγa, RPTPγb	RPTPγ	R5	–	Coronary artery disease; QT interval; Inflammation	+	+
ptprh	sap1	SAP1	R3	–	–	–	–
ptprja, ptprjb	dep1a, dep1b	DEP1	R3	Arterial venous cell fate decision [39]	Thyroid cancer; Precursor cell lymphoblastic leukemia	+++	–
ptprk	RPTPκ	RPTPκ	R2A	–	Celiac disease; Albuminuria	–	–
ptprm	RPTPμ	RPTPμ	R2A	–	Prostatic neoplasms; Fibrinogen	–	–
ptprna, ptprnb	IA2a, IA2b	IA2	R8	–	–	+	+
ptprn2	IA2β	IA2β	R8	–	Mental disorders; Albumins	+++	++
ptpro	GLEPP	GLEPP1	R3	Cerebellar formation [34]	Mental processes; Body mass index	–	+
ptprq	PTPS31	PTPS31	R3	–	Bipolar disorder; Erythrocyte indices; Electrocardiography	–	–
ptprr	pcPTP	PCPTP	R7	–	Parkinson disease	–	–
ptprsa, ptprsb	RPTPσa, RPTPσb	RPTPσ	R2B	Synaptic vesicles [7]	Alcoholism	++	++ (knockin)
ptprt	RPTPρ	RPTPρ	R2A	–	Depressive disorder; Diabetes mellitus;	+++	++++
ptprua, ptprub	RPTPλa, RPTPλb	RPTPλ	R2A	Gastrulation [1]	Heart failure; Bipolar disorder; Diabetes mellitus, Type 2	+	–
ptprza, ptprzb	RPTPζa, RPTPζb	RPTPζ	R5	–	Cholesterol, LDL	++	–
ptena, ptenb	Ptena, Ptenb	PTEN	DSP	Early development [14], hemangiosarcoma [7]	Hemangiosarcoma; Prostate cancer	++	++

mutations or insertions at will. Successful homologous recombination in zebrafish using TALENs to introduce an exogenous restriction site or loxP sites has been reported [5].

5. PTPs in zebrafish gastrulation cell movements

Several PTPs have an essential role in gastrulation cell movements, in particular convergence and extension (C&E) cell movements. These morphogenetic cell movements shape the developing zebrafish embryo [41]. Cell movements in the developing embryo were determined by *in toto* imaging using light sheet microscopy, which provides a stunning view of gastrulation cell movements and at the same time illustrates the strength of the zebrafish as a model for intravital imaging [26]. Signaling has a crucial role in gastrulation cell movements and we and others found that several PTPs are essential for C&E cell movements. Knockdown of Shp2 results in defective gastrulation cell movements, without affecting cell fate specification [25]. RPTPα and PTPε are also required for normal gastrulation cell movements.

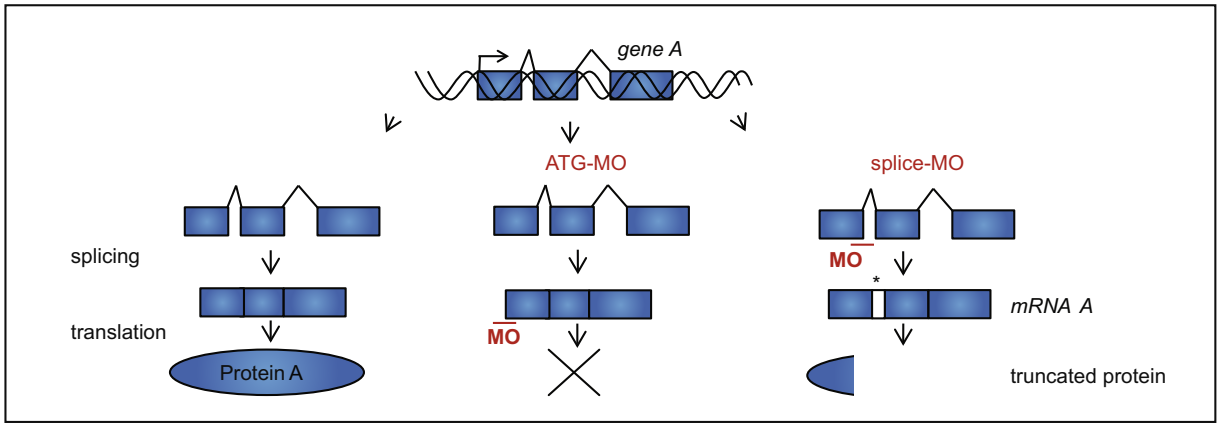

Fig. 1. Morpholino method. Both translation initiation and splice-site blocking morpholinos have been used to knockdown expression of target proteins. Gene A is transcribed and the RNA is spliced and translated normally. Translation initiation blocking morpholinos (ATG-MO) are targeted at the start ATG and will interfere with mRNA binding to the ribosome complex thus leading to impaired protein synthesis of Protein A. Splice-site blocking morpholinos (splice-MO) are targeted at splice-donor or -acceptor sites and interfere with splicing, thus leading to inclusion of introns which may contain internal stop sites or lead to a frame shift, resulting in truncated, dysfunctional proteins.

Transient morpholino-mediated knockdown of RPTPα and PTPε, but also a genetic mutant of *ptpra* display C&E cell movement defects [45]. Moreover, knockdown of RPTPψ results in defects in C&E cell movements during gastrulation [1]. Finally, knockdown of PTP-BL and Ptpn20 induces gastrulation cell movement defects [46].

Not only knockdowns of PTPs induce gastrulation cell movement defects, but also expression of mutant Shp2 with mutations that were identified in human patients with Noonan Syndrome or LEOPARD syndrome display C&E cell movement defects. These embryos display defects at later stages that are reminiscent of the symptoms observed in human patients, including short stature, hypertelorism and cardiac defects [25]. Interestingly, expression of LEOPARD mutant Shp2 induces defects in neural crest specification and migration [42]. It remains to be determined how an activating mutation (Noonan Syndrome), an inactivating mutation (LEOPARD syndrome) and a knockdown induce similar developmental defects in early embryonic development.

PTP signaling, resulting in gastrulation cell movements, was investigated by analysis of genetic epistasis interactions. Particularly, we studied the role of Src family kinases, because these are activated by PTPs and have a role in C&E cell movements [23,24], and Rho family GTPases, because these are downstream regulators of gastrulation cell movements [15]. Partial knockdown of Shp2, RPTPα or PTPε does not affect development, nor does partial knockdown of the Src family kinases, Fyn and Yes, but combined partial knockdown of these PTPs and Src family kinases induces severe gastrulation cell movement defects [25,45], indicating a genetic interaction. RhoA, but not Rac was identified to act downstream of Src family kinases in gastrulation cell movements [23]. Constitutively active RhoA rescues Shp2, RPTPα and PTPε knockdowns [25,45], which provides insight into the mechanism underlying PTP signaling in gastrulation cell movements. Intriguingly, the PTP-BL and ptpn20 knockdowns are rescued by dominant negative RhoA, in contrast to the RPTPα and PTPε knockdowns. We suggest a model in which PTPs regulate cell polarization, which is at the basis of normal C&E cell movements during gastrulation [46]. Some PTPs have positive effects on cell polarization and others negatively affect polarization. Both effects result in decreased directed cell migration and hence to defective C&E cell movements. Many PTPs are essential for normal C&E cell movements, which probably reflects the high level of regulation of C&E cell movements. Detailed analysis of the role of each PTP in C&E cell movements will provide insight into the interplay between PTPs – if any – in the regulation of C&E cell movements.

6. Quantitative analysis of gastrulation defects

While analyzing gastrulation cell movement defects in zebrafish embryos we developed assays to quantitatively determine defective cell movements, based on (1) the shape of the embryo, (2) molecular markers and (3) cell migration.

6.1. Detecting oval-shaped embryos

Defective cell movements during epiboly and gastrulation lead to oval-shaped embryos [3,40]. Using Image J, we have developed a semi-automated tool to determine the oval shape of embryos. The circumference of the embryo is detected and subsequently, the long axis and perpendicular to that the short axis is determined (Fig. 2A). The ratio long axis/short axis directly represents the extent of oval shape. Wild type non-injected embryos display a ratio of 1.1, i.e. close to 1.0, the perfect sphere. The ratios of embryos with epiboly defects are usually 1.3 and up, significantly higher than 1.1 in wildtype and control-injected embryos. Interestingly, CI-1040, a specific inhibitor of MEK, which acts downstream in the pathway rescues the oval shape of the embryos, whereas it does not affect the ratio of wildtype embryos [40]. Detecting oval shapes of zebrafish embryos is a straightforward method to quantitatively determine the deviation from the normal shape of control embryos and therefore the severity of gastrulation defects.

6.2. Molecular markers

Embryos with C&E cell movement defects are characterized by a broader body and reduced extension of the body axis. Cell fate is not affected by defects in C&E cell movements and all cell types that are normally observed in the developing embryo are detectable in embryos with defective gastrulation cell movements. We routinely use a panel of markers to assess that cell fate is not affected. These include markers for: the dorsal organizer (*goosecoid, gsc*), ventral cell fate (*bone morphogenetic protein 2b*, *bmp2b*), dorsalizing factor (*chordin*, *chd*) and mesendoderm (*notail*, *ntl*) at shield stage; axial mesendoderm at 70% epiboly (*cyclops*, *cyc*) and at budstage forebrain (*six3*) and mid-hindbrain boundary (*pax2*). Several markers have been identified that provide quantifiable traits of C&E cell movements in the developing embryo at early developmental stages. *Dlx3* (currently known as *dlx3b*) marks the edges of the neural plate and *hgg1* (current name *ctsl1b*) marks

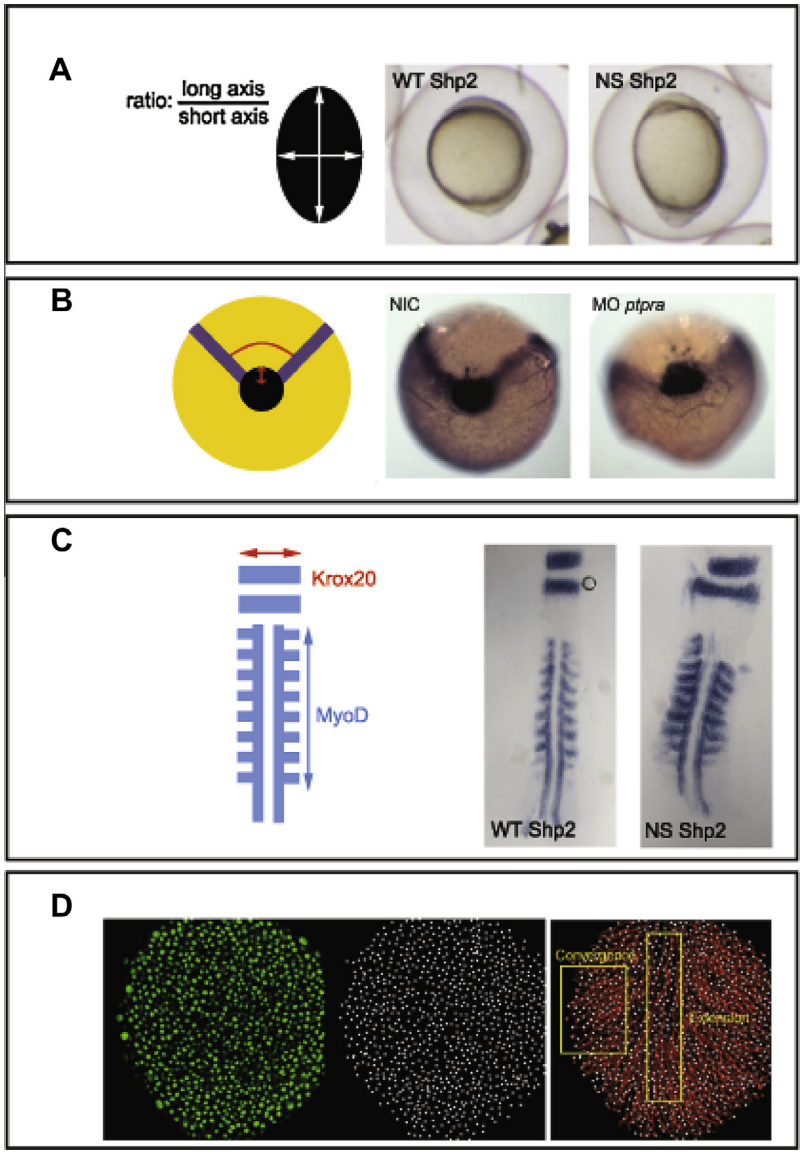

Fig. 2. Quantitative analysis of defects in gastrulation cell movements. (A) Assessment of oval shape, (B) the width and relative position of molecular markers, *dlx3* and *hgg1* (currently known as *dlx3b* and *ctsl1b*, respectively), (C) the length and width of the developing embryo using molecular markers, *krox20* and *myod* and (D) migration of mesendodermal cells in the developing embryo can all be used as quantitative traits of C&E cell movements. In A–C a schematic representation is given next to an actual comparison of a control embryo (wildtype Shp2 injected, WT Shp2, or non-injected control, NIC) and an experimental embryo (Noonan Shp2 injected, NS Shp2, or *ptpra* morpholino-injected). In panel D the actual confocal image is compared to the image after processing. The right panel shows the cell tracks. Cell movements in the boxed areas are directly proportional to convergence (Con) and extension (Ext) cell movements, respectively. See text for details.

precursors of the hatching gland. Double labeling with *dlx3* and *hgg1* provides a characteristic pattern (Fig. 2B). The position of the hatching gland, relative to the anterior-most *dlx3* staining provides a direct measure for body axis extension and the angle of the *dlx3*-positive edges of the neural plate are directly representative of convergence [45]. In embryos with defective C&E cell movements, the *hgg1* staining is located more posteriorly and the *dlx3* staining is significantly wider (Fig. 2B).

Krox20/myod double labeling at the 8–10 somite stage and subsequent flat-mounting of the embryos leads to a highly reproducible pattern that can be used for quantification of the width and length of the embryo [33] (Fig. 2C). The *krox20* marker stains rhombomeres 3 and 5 and *myod* marks the somites. Embryos with 8–10 somites are used, and staining of the somites provides a good means to determine the age of the embryos, as a new somite is added every 30 min at this stage. The distance from the first to the eighth somite remains identical from the 8-somite to the 10-somite stage. The width of the *krox20*-positive rhombomere 3 and the length of somites 1–8 are directly proportional to the width and length of the embryo, respectively, and the ratio of width and length allows direct quantitative comparison between groups of experimental embryos.

6.3. Cell migration

Identification of differences in the migration of paraxial mesendodermal cells between groups of embryos is definitive evidence for differences in C&E cell movements. Initially, we used a photoactivatable dye, 4,5-dimethoxy-2-nitrobenzyl (DMND)-caged fluorescein dextran (10,000 MW; Molecular Probes, Leiden, the Netherlands) that was uncaged by local illumination with UV light at 6 hpf as described [4]. The fluorescent group of cells was subsequently followed using an Axioplan microscope, equipped with a UV light source, adjustable pinhole and 40X objective. Either a

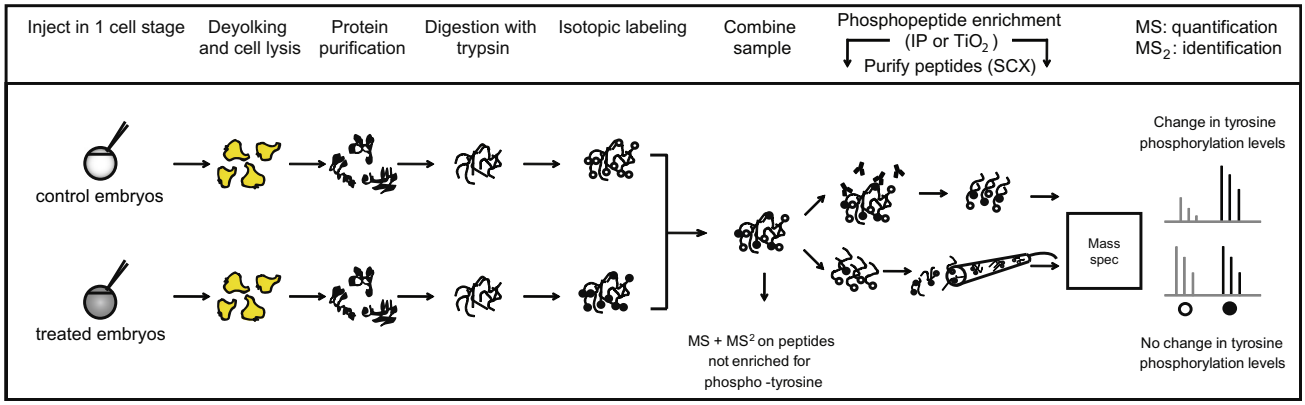

Fig. 3. Phosphoproteomics analysis of zebrafish embryos. Zebrafish embryos (control and/or treated) are deyolked to remove excess yolk proteins which would otherwise interfere with mass spectrometric analysis. Embryos are lysed and proteins are purified and digested with trypsin. For quantification, we have used isotopic dimethyl labeling. Samples are then combined for direct analysis (reference pool of all peptides) and the samples are used for further processing. To enrich for phosphopeptides, either anti-pTyr immunoprecipitation or TiO_2 enrichment (for pSer, pThr and pTyr) are being used. Fractionation of peptides is performed using strong cation exchange after (pTyr IP) or prior to (TiO_2) phosphopeptide enrichment. Mass spectrometric analysis is performed to quantify (MS) and identify (MS_2) peptides of interest. See text for further details.

group of cells in the embryo proper was photo-activated, allowing assessment of extension, or a group of mesendodermal cells was labeled, allowing assessment of convergence. Pictures were taken immediately following uncaging (6 hpf), at 80% epiboly (8 hpf) and at tailbud stage (10 hpf). As a measure for cell migration, the angles for dorsal convergence and anterior extension were determined using Image J software. Knockdown of Shp2 and expression of Noonan Syndrome mutant Shp2 induced significant defects in C&E cell movements, assessed using a caged fluorophore as described above [23].

We developed an alternative for these photo-activation experiments: time-lapse imaging of mesendodermal cells during gastrulation [45]. Briefly, all nuclei of a developing embryo are labeled by microinjection at the one-cell stage with fluorescently labeled Histone 1 protein (Histone 1 Alexa fluor 488; Molecular Probes). The embryos are dechorionated at 30% epiboly and mounted at shield stage in 1% low melting point agarose with the dorsal side against the coverslip approximately 100 μm anterior to shield position, facilitating visualization of the C&E cell movements of the epiblast. We use a Leica SP2 confocal microscope with a 40x objective and a 488 nm laser line for excitation of the fluorophore. Images are recorded every 2 min from shield stage until 1-somite stage. The timelapse images are analyzed using Image J software. The nuclear Histone 1 labeling is used to determine the position of individual nuclei in a single optical slice for each time point. Due to innate changes in intensity, size and shape of the fluorescent signal of the nuclei, additional image processing is needed for efficient tracing of the cells. The images are successively made binary, separated by a water shedding algorithm, eroded to a single pixel and dilated. Projection of the resulting image onto the original shows that the generated objects represent cell positions with a very high accuracy (>99%) (Fig. 2D). These objects are readily traced over time, which generates a report with the Cartesian coordinates for all traced objects at each time point. These coordinates represent the contribution of cell migration to convergence (*X*-axis) and extension (*Y*-axis) and allow for quantification of migration of individual cells and of groups of cells. We have used this cell tracking method to compare C&E cell movements between wild type and *ptpra*$^{-/-}$ mutant embryos that lack functional RPTPα. *Ptpra*$^{-/-}$ embryos display significantly impaired C&E cell movements [45]. The latter cell tracking method does not rely on the use of a caged fluorophore, but instead a general cell identifier can be used. We have used fluorescently labeled Histone 1 for our experiments as well as a transgenic line, expressing nuclear GFP, with similar results [40].

7. Phosphoproteomics in zebrafish

The methods above facilitate the analysis of PTP function at the organismal and cellular level. Biochemical analyses are required to understand the function of PTPs at the molecular level. Whereas the zebrafish is an excellent model system to unravel genetic pathways, biochemical analyses are lagging behind due to ill-understood difficulties in the use of antibodies in zebrafish lysates, even though the epitopes of the antibodies that are being used are highly or even perfectly conserved. Highly abundant yolk proteins are likely to interfere with protein analyses in zebrafish lysates, yet some antibodies work remarkably well in immunoblots and immunoprecipitation. Nevertheless, phosphoproteomic analysis of zebrafish embryos by mass spectrometry has provided some insight into the overall phosphoproteome of zebrafish embryos and may provide means to analyze the function of PTPs *in vivo* at the phosphoprotein level. As a first step to analyze PTP function at the molecular level *in vivo*, we set out to map the pTyr phosphoproteome in zebrafish embryos by anti-pTyr immunoprecipitation and mass spectrometry to identify phosphoproteins and protein phosphorylation sites [32]. In the process, we developed a protocol for quantitative phosphoproteomic analyses of zebrafish embryos: First, embryos are collected and excess yolk proteins are removed by washing with ice-cold deyolking buffer (Fig. 3). The deyolked embryos may be snap-frozen until a sufficient amount of sample has been collected. Labeling of zebrafish embryos, similar to tissue culture cells with stable isotope labeling in culture (SILAC) is not feasible. Therefore, in order to compare different samples with eachother, peptides are labeled, either using iTRAQ or using stable isotope containing dimethyl [30]. While iTRAQ allows for a comparison of up to eight different conditions, dimethyl labeling is cost-effective and facilitates a comparison of up to three different samples. Purification of the sample is performed using either TiO_2 columns which enrich for all phosphorylated peptides, or by pTyr-specific immunoprecipitation. Note that for pTyr immunoprecipitation collection of more sample (preferably >6 μg, or more than 2000 zebrafish embryos) is necessary than for TiO_2. In contrast to pTyr immunoprecipitation, TiO_2 can be used to purify all phosphopeptides and to analyze the phosphoproteome in relatively small samples, down to a single zebrafish embryo [31]. Using the TiO_2 approach, we successfully analyzed the phosphoproteome of Fyn/Yes knockdown embryos that exhibit gastrulation cell movement defects [30]. Future analysis specifically of the pTyr phosphoproteome of PTP knockdown or knockout embryos by

immunoprecipitation of pTyr-containing peptides after proteolysis and subsequent peptide identification by mass spectrometry may lead to identification of direct substrates and elucidate PTP-proximal signaling.

8. Outlook

Here we describe genetic methods to manipulate gene function in zebrafish with the emphasis on PTPs. We explain how zebrafish can be used to study PTP function using a variety of quantitative methods to study general morphology and cell migration. Furthermore, we provide an overview of PTP studies performed in zebrafish and the genetic mutants available. In Table 1 we show that several PTPs have been studied in zebrafish, however, many are yet to be investigated. Additionally, genetic association studies have shown a role for PTPs in several diseases. Combined with the availability of genetic mutants this holds a big promise for zebrafish as tools to study PTPs. In addition, the advent of TALEN and CRISPR technology has facilitated the generation of targeted genetic mutations in the zebrafish genome and many more zebrafish mutants will be generated in the near future in which genes encoding PTPs are inactivated or contain mutations at specific positions. These genetic mutations will be crossed with transgenic lines in which fluorescent proteins are expressed in specific cells or tissues, allowing analysis of cell behavior *in vivo* by intravital imaging, thus providing insight into the function of PTPs at the cellular/organismal level. Analysis of the pTyr phosphoproteome of zebrafish embryos that lack the function of a specific PTP or that express mutant PTPs may result in identification of specific substrates and signaling pathways, thus providing insight into the function of PTPs at the molecular level *in vivo*. Using these methods, the zebrafish provides great opportunities to study PTP function in development and disease *in vivo*.

References

[1] B. Aerne, D. Ish-Horowicz, Development 131 (2004) 3391–3399.
[2] A. Alonso, J. Sasin, N. Bottini, I. Friedberg, A. Osterman, A. Godzik, T. Hunter, J. Dixon, T. Mustelin, Cell. 117 (2004) 699–711.
[3] C. Anastasaki, A.L. Estep, R. Marais, K.A. Rauen, E.E. Patton, Hum. Mol. Genet. 18 (2009) 2543–2554.
[4] J. Bakkers, C. Kramer, J. Pothof, N.E. Quaedvlieg, H.P. Spaink, M. Hammerschmidt, Development 131 (2004) 525–537.
[5] V.M. Bedell, Y. Wang, J.M. Campbell, T.L. Poshusta, C.G. Starker, R.G. Krug 2nd, W. Tan, S.G. Penheiter, A.C. Ma, A.Y. Leung, S.C. Fahrenkrug, D.F. Carlson, D.F. Voytas, K.J. Clark, J.J. Essner, S.C. Ekker, Nature 491 (2012) 114–118.
[6] S. Carra, E. Foglia, S. Cermenati, E. Bresciani, C. Giampietro, C. Lora Lamia, E. Dejana, M. Beltrame, F. Cotelli, PLoS One 7 (2012) e51245.
[7] J. Chen, G. Lee, A.H. Fanous, Z. Zhao, P. Jia, A. O'Neill, D. Walsh, K.S. Kendler, X. Chen, Schizophr. Res. 131 (2011) 43–51.
[8] X. Chen, T. Yoshida, H. Sagara, Y. Mikami, M. Mishina, J. Neurochem. 119 (2011) 532–543.
[9] S. Choorapoikayil, R.V. Kuiper, A. de Bruin, J. den Hertog, Dis. Model Mech. 5 (2012) 241–247.
[10] S. Choorapoikayil, J. Overvoorde, J. den Hertog, Deriving cell lines from zebrafish embryos and tumors, Zebrafish, in press, http://dx.doi.org/10.1089/zeb.2013.0866
[11] J. den Hertog, Biosci. Rep. 25 (2005) 289–297.
[12] Y. Doyon, J.M. McCammon, J.C. Miller, F. Faraji, C. Ngo, G.E. Katibah, R. Amora, T.D. Hocking, L. Zhang, E.J. Rebar, P.D. Gregory, F.D. Urnov, S.L. Amacher, Nat. Biotechnol. 26 (2008) 702–708.
[13] W. Driever, L. Solnica-Krezel, A.F. Schier, S.C. Neuhauss, J. Malicki, D.L. Stemple, D.Y. Stainier, F. Zwartkruis, S. Abdelilah, Z. Rangini, J. Belak, C. Boggs, Development 123 (1996) 37–46.
[14] A. Faucherre, G.S. Taylor, J. Overvoorde, J.E. Dixon, J. den Hertog, Oncogene 27 (2008) 1079–1086.
[15] R. Habas, I.B. Dawid, X. He, Genes Dev. 17 (2003) 295–309.
[16] P. Haffter, M. Granato, M. Brand, M.C. Mullins, M. Hammerschmidt, D.A. Kane, J. Odenthal, F.J. van Eeden, Y.J. Jiang, C.P. Heisenberg, R.N. Kelsh, M. Furutani-Seiki, E. Vogelsang, D. Beuchle, U. Schach, C. Fabian, C. Nusslein-Volhard, Development 123 (1996) 1–36.
[17] M. Hayashi, A. Majumdar, X. Li, J. Adler, Z. Sun, S. Vertuani, C. Hellberg, S. Mellberg, S. Koch, A. Dimberg, G.Y. Koh, E. Dejana, H.G. Belting, M. Affolter, G. Thurston, L. Holmgren, D. Vestweber, L. Claesson-Welsh, Nat. Commun. 4 (2013) 1672.
[18] W.J. Hendriks, A. Elson, S. Harroch, R. Pulido, A. Stoker, J. den Hertog, FEBS J. 280 (2013) 708–730.
[19] W.J. Hendriks, A. Elson, S. Harroch, A.W. Stoker, FEBS J. 275 (2008) 816–830.
[20] K. Howe, M.D. Clark, C.F. Torroja, J. Torrance, C. Berthelot, M. Muffato, J.E. Collins, S. Humphray, K. McLaren, L. Matthews, S. McLaren, I. Sealy, M. Caccamo, C. Churcher, C. Scott, J.C. Barrett, R. Koch, G.J. Rauch, S. White, W. Chow, B. Kilian, L.T. Quintais, J.A. Guerra-Assuncao, Y. Zhou, Y. Gu, J. Yen, J.H. Vogel, T. Eyre, S. Redmond, R. Banerjee, J. Chi, B. Fu, E. Langley, S.F. Maguire, G.K. Laird, D. Lloyd, E. Kenyon, S. Donaldson, H. Sehra, J. Almeida-King, J. Loveland, S. Trevanion, M. Jones, M. Quail, D. Willey, A. Hunt, J. Burton, S. Sims, K. McLay, B. Plumb, J. Davis, C. Clee, K. Oliver, R. Clark, C. Riddle, D. Eliott, G. Threadgold, G. Harden, D. Ware, B. Mortimer, G. Kerry, P. Heath, B. Phillimore, A. Tracey, N. Corby, M. Dunn, C. Johnson, J. Wood, S. Clark, S. Pelan, G. Griffiths, M. Smith, R. Glithero, P. Howden, N. Barker, C. Stevens, J. Harley, K. Holt, G. Panagiotidis, J. Lovell, H. Beasley, C. Henderson, D. Gordon, K. Auger, D. Wright, J. Collins, C. Raisen, L. Dyer, K. Leung, L. Robertson, K. Ambridge, D. Leongamornlert, S. McGuire, R. Gilderthorp, C. Griffiths, D. Manthravadi, S. Nichol, G. Barker, S. Whitehead, M. Kay, et al., Nature 496 (2013) 498–503.
[21] W.Y. Hwang, Y. Fu, D. Reyon, M.L. Maeder, S.Q. Tsai, J.D. Sander, R.T. Peterson, J.R. Yeh, J.K. Joung, Nat. Biotechnol. 31 (2013) 227–229.
[22] O. Jaillon, J.M. Aury, F. Brunet, J.L. Petit, N. Stange-Thomann, E. Mauceli, L. Bouneau, C. Fischer, C. Ozouf-Costaz, A. Bernot, S. Nicaud, D. Jaffe, S. Fisher, G. Lutfalla, C. Dossat, B. Segurens, C. Dasilva, M. Salanoubat, M. Levy, N. Boudet, S. Castellano, V. Anthouard, C. Jubin, V. Castelli, M. Katinka, B. Vacherie, C. Biemont, Z. Skalli, L. Cattolico, J. Poulain, V. De Berardinis, C. Cruaud, S. Duprat, P. Brottier, J.P. Coutanceau, J. Gouzy, G. Parra, G. Lardier, C. Chapple, K.J. McKernan, P. McEwan, S. Bosak, M. Kellis, J.N. Volff, R. Guigo, M.C. Zody, J. Mesirov, K. Lindblad-Toh, B. Birren, C. Nusbaum, D. Kahn, M. Robinson-Rechavi, V. Laudet, V. Schachter, F. Quetier, W. Saurin, C. Scarpelli, P. Wincker, E.S. Lander, J. Weissenbach, H. Roest Crollius, Nature 431 (2004) 946–957.
[23] C. Jopling, J. den Hertog, EMBO Rep. 6 (2005) 426–431.
[24] C. Jopling, J. den Hertog, Mech. Dev. 124 (2007) 129–136.
[25] C. Jopling, D. van Geemen, J. den Hertog, PLoS Genet. 3 (2007) e225.
[26] Z. Kanwal, A. Zakrzewska, J. den Hertog, H.P. Spaink, M.J. Schaaf, A.H. Meijer, J. Immunol. 190 (2013) 1631–1645.
[27] P.J. Keller, A.D. Schmidt, J. Wittbrodt, E.H. Stelzer, Science 322 (2008) 1065–1069.
[28] R.N. Kettleborough, E.M. Busch-Nentwich, S.A. Harvey, C.M. Dooley, E. de Bruijn, F. van Eeden, I. Sealy, R.J. White, C. Herd, I.J. Nijman, F. Fenyes, S. Mehroke, C. Scahill, R. Gibbons, N. Wali, S. Carruthers, A. Hall, J. Yen, E. Cuppen, D.L. Stemple, Nature 496 (2013) 494–497.
[29] Z. Lele, J. Bakkers, M. Hammerschmidt, Genesis 30 (2001) 190–194.
[30] S. Lemeer, C. Jopling, J. Gouw, S. Mohammed, A.J. Heck, M. Slijper, J. den Hertog, Mol. Cell. Proteomics 7 (2008) 2176–2187.
[31] S. Lemeer, M.W. Pinkse, S. Mohammed, B. van Breukelen, J. den Hertog, M. Slijper, A.J. Heck, J. Proteome Res. 7 (2008) 1555–1564.
[32] S. Lemeer, R. Ruijtenbeek, M.W. Pinkse, C. Jopling, A.J. Heck, J. den Hertog, M. Slijper, Mol. Cell. Proteomics 6 (2007) 2088–2099.
[33] C. Li, P.N. Inglis, C.C. Leitch, E. Efimenko, N.A. Zaghloul, C.A. Mok, E.E. Davis, N.J. Bialas, M.P. Healey, E. Heon, M. Zhen, P. Swoboda, N. Katsanis, M.R. Leroux, PLoS Genet. 4 (2008) e1000044.
[34] W.H. Liao, C.H. Cheng, K.S. Hung, W.T. Chiu, G.D. Chen, P.P. Hwang, S.P. Hwang, Y.S. Kuan, C.J. Huang, Cell. Mol. Life Sci. 70 (2013) 2367–2381.
[35] G.J. Lieschke, P.D. Currie, Nat. Rev. Genet. 8 (2007) 353–367.
[36] X. Meng, M.B. Noyes, L.J. Zhu, N.D. Lawson, S.A. Wolfe, Nat. Biotechnol. 26 (2008) 695–701.
[37] A. Nasevicius, S.C. Ekker, Nat. Genet. 26 (2000) 216–220.
[38] R.T. Peterson, B.A. Link, J.E. Dowling, S.L. Schreiber, Proc. Natl. Acad. Sci. USA 97 (2000) 12965–12969.
[39] F. Rodriguez, A. Vacaru, J. Overvoorde, J. den Hertog, Dev. Biol. 324 (2008) 122–130.
[40] V. Runtuwene, M. van Eekelen, J. Overvoorde, H. Rehmann, H.G. Yntema, W.M. Nillesen, A. van Haeringen, I. van der Burgt, B. Burgering, J. den Hertog, Dis. Model Mech. 4 (2011) 393–399.
[41] L. Solnica-Krezel, Curr. Opin. Genet. Dev. 16 (2006) 433–441.
[42] R.A. Stewart, T. Sanda, H.R. Widlund, S. Zhu, K.D. Swanson, A.D. Hurley, M. Bentires-Alj, D.E. Fisher, M.I. Kontaridis, A.T. Look, B.G. Neel, Dev. Cell 18 (2010) 750–762.
[43] C. Thisse, B. Thisse, Nat. Protoc. 3 (2008) 59–69.
[44] N.K. Tonks, FEBS J. 280 (2013) 346–378.
[45] M. van Eekelen, J. Overvoorde, C. van Rooijen, J. den Hertog, PLoS One 5 (2010) e12573.
[46] M. van Eekelen, V. Runtuwene, W. Masselink, J. den Hertog, PLoS One 7 (2012) e35913.
[47] M. van Eekelen, V. Runtuwene, J. Overvoorde, J. den Hertog, Dev. Biol. 340 (2010) 626–639.
[48] K. Vandepoele, W. De Vos, J.S. Taylor, A. Meyer, Y. Van de Peer, Proc. Natl. Acad. Sci. USA 101 (2004) 1638–1643.
[49] D. Wang, L.E. Jao, N. Zheng, K. Dolan, J. Ivey, S. Zonies, X. Wu, K. Wu, H. Yang, Q. Meng, Z. Zhu, B. Zhang, S. Lin, S.M. Burgess, Proc. Natl. Acad. Sci. USA 104 (2007) 12428–12433.
[50] F. Wang, S.N. Wolfson, A. Gharib, A. Sagasti, Curr. Biol. 22 (2012) 373–382.
[51] E. Wienholds, S. Schulte-Merker, B. Walderich, R.H. Plasterk, Science 297 (2002) 99–102.
[52] L. Wyatt, C. Wadham, L.A. Crocker, M. Lardelli, Y. Khew-Goodall, J. Cell Biol. 178 (2007) 1223–1235.